The Astrophysical Journal Letters, 738:L3 (6pp), 2011 September 1 doi:10.1088/2041-8205/738/1/L3

ULTRAVIOLET PHOTON-INDUCED SYNTHESIS AND TRAPPING OF H_2O_2 AND O_3 IN POROUS WATER ICE FILMS IN THE PRESENCE OF AMBIENT O_2: IMPLICATIONS FOR EXTRATERRESTRIAL ICE

J. Shi[1], U. Raut[1], J.-H. Kim[1], M. Loeffler[2], and R. A. Baragiola[1,3]
[1] Laboratory of Atomic and Surface Physics, University of Virginia, Charlottesville, VA 22904, USA; raul@virginia.edu
[2] Goddard Space Flight Center, Greenbelt, MD 20771, USA
Received 2011 June 23; accepted 2011 July 15; published 2011 August 8

ABSTRACT

The mass uptake of ambient oxygen in nanoporous ice is enhanced by irradiation with 193 nm photons, due to conversion of O_2 into H_2O_2 and O_3, with an efficiency that increases with decreasing temperature. These findings show a new way to form H_2O_2 and O_3 on icy surfaces in the outer solar system at depths much larger than are accessible by typical ionizing radiation, with possible astrobiological implications.

Key words: atomic processes – methods: laboratory – planets and satellites: atmospheres – planets and satellites: surfaces – radiation mechanisms: general

Online-only material: color figures

1. INTRODUCTION

Water ice is a major constituent of most icy surfaces in the outer solar system, where it is bombarded by the solar wind, magnetospheric ions, cosmic rays, and micrometeorites. Radiation chemistry occurs when energetic radiation dissociates the water molecules into H, OH, O, and H_2. Scattering of dissociation products by surrounding molecules (the "cage") often leads to recombination back into H_2O (Hardwick 1952). The lighter H receives most of the kinetic energy during dissociation which, together with its small size, makes it the most likely product to escape the cage. Subsequent formation of H_2 and its diffusion out of the ice lead to an O-rich solid containing mostly water and small amounts of trapped radicals such as OH, H, O, and HO_2. Irradiation results in the formation of O_2 and H_2O_2 through a series of radical reactions. The O_2 can leave the ice by irradiation-enhanced desorption (Teolis et al. 2005) or thermally desorb above ∼130 K (Teolis et al. 2005).

Remote sensing of icy satellites has revealed condensed O_2 on Ganymede (Spencer et al. 1995; Calvin et al. 1996), Europa, Callisto (Spencer & Calvin 2002), and inferred it at Rhea (Teolis et al. 2010), and is believed to be a radiolytic products of H_2O (Spencer et al. 1995; Spencer & Calvin 2002) and H_2O_2 (Carlson et al. 1999; Hendrix et al. 1999). Condensed ozone may have been identified on Ganymede (Noll et al. 1996) through a broad absorption band in the ultraviolet that is similar to the O_3 Hartley absorption band at 260 nm. However, other molecules absorb in this wavelength range, making this assignment and a similar one for the Saturnian satellites Dione and Rhea (Noll et al. 1997) less compelling. Johnson & Jesser (1997) hypothesized that O_3 was formed from O_2 trapped in bubbles that had been produced by radiolysis of the surface ice. Initial experiments showed that although trapped oxygen is produced by radiolysis (Bahr et al. 2001; Teolis et al. 2005), the amount is insufficient to account for the observations of condensed O_2 and O_3. However, ensuing laboratory studies showed that if the irradiation occurred together with deposition of water, which mimicked the gravitational return of desorbed molecules to the surface (Teolis et al. 2006), then the amount of trapped O_2 in the sample could be significantly increased and O_3 could be synthesized.

This remarkable finding led us to speculate that these synergistic effects could be significant for other icy body environments as well. Thus, in an effort to simulate closely the conditions on icy satellites and rings, where an oxygen exosphere and energetic bombardment of the surface coexist (Shi et al. 2009), we irradiated water ice with energetic protons in the presence of ambient O_2. Under these conditions, we found that O_2 adsorption and trapping were enhanced, due to increase in the number of adsorption sites with higher binding energy and simultaneous ion-induced ice compaction (Raut et al. 2007). These findings contrasted well with our other results (Shi et al. 2009) that showed O_2 adsorption onto microporous ice films was reversible if irradiation was absent, i.e., the O_2 completely desorbs upon removal of the ambient O_2.

Such radiation-induced physical and chemical processes should also occur under energetic electron and photon impact since these types of radiation are known to alter the structure of ice (Baragiola 2003). Unlike typical magnetospheric ions, ultraviolet (UV) photons are limited in the type of molecule they can dissociate. In this Letter, we investigate the effect of 193 nm photon irradiation of porous ices in the presence of ambient O_2, using infrared spectroscopy, thermal desorption spectroscopy, and microbalance gravimetry. UV photons at this and higher wavelengths that can dissociate molecules, such as oxygen, are important on icy surfaces since these photons can penetrate much deeper in the regolith than magnetospheric ions, due to their negligible absorption cross section in water ice. Effects of such photons may dominate around Saturn where the magnetospheric energy flux is significantly smaller than at Jupiter's moons.

2. EXPERIMENTAL SETUP AND PROCEDURES

The experiments were conducted in an ultrahigh vacuum (UHV) chamber with a base pressure of 10^{-10} mbar. Water ice films were vapor deposited onto a gold-coated quartz crystal microbalance (QCM) through a collimating microcapillary array doser at an incidence of 45°. The films were first grown at 70 K, then warmed or cooled to temperatures between 40 K and 80 K.

[3] Corresponding author.

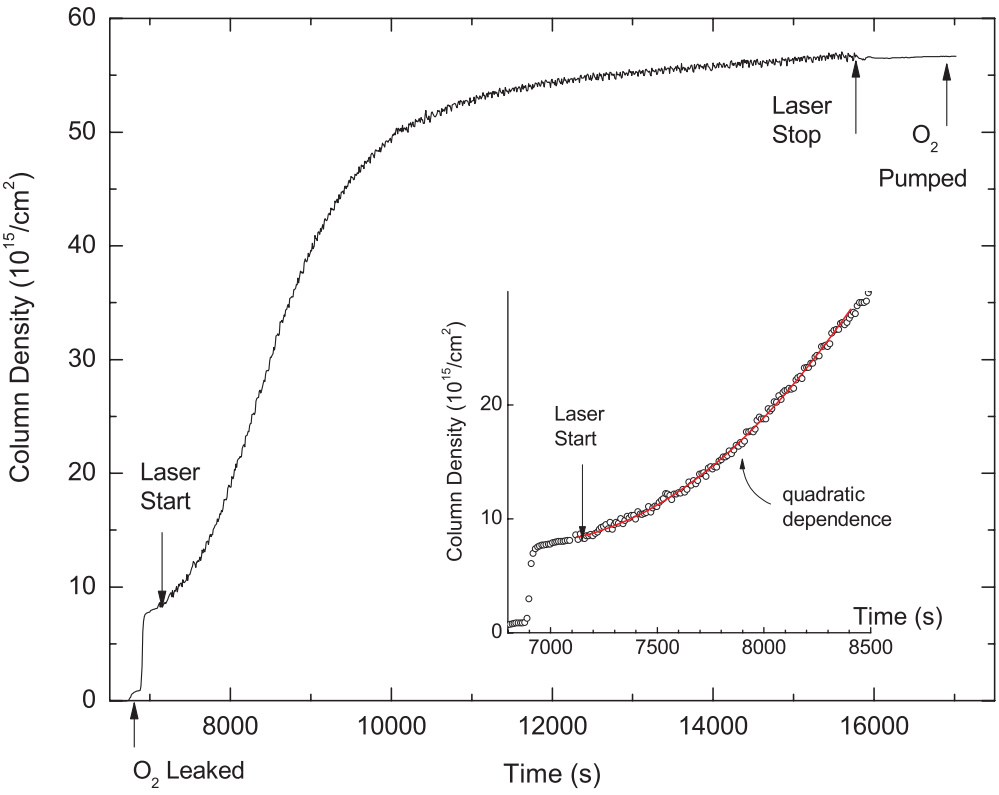

Figure 1. Column density of O_2 adsorbed by the 1600 monolayer ice film during O_2 and UV exposure at 50 K. Irradiation of the film with 193 nm laser light started following O_2 adsorption equilibrium, to a total fluence of 4.3×10^{19} photons cm^{-2}. Inset: magnified initial stage of laser irradiation to emphasize the initial quadratic dependence on time.

(A color version of this figure is available in the online journal.)

The porosity of the films was ∼21%, measured by spectroscopic interferometry (Shi et al. 2009). The areal mass of the deposited films was measured from the change of the resonant frequency of the microbalance (Sack & Baragiola 1993) and converted to column density by dividing by the mass of the water molecule. All films used in this Letter were deposited to a column density of 1600 ML (1 ML = 10^{15} molecules cm^{-2}).

Light pulses from an ArF excimer laser with a wavelength of 193 nm, operated at 5 Hz, was defocused by a lens and passed through a window in the vacuum chamber onto the sample. The defocused beam provided uniform irradiation over the sensitive area of the microbalance. The average flux at the position of the microbalance, measured with a calibrated photodetector, was 3.4×10^{14} photons cm^{-2} s^{-1}. Such a low flux did not cause significant multi-photon absorption or sample heating. O_2, N_2, and Ar gases were introduced into the chamber and maintained at a constant pressure prior to irradiation. Mass changes were monitored by the microbalance during experiments. We note that in all experiments reported we observe that 2–6 ML of CO_2 was adsorbed to our sample during photolysis, which is likely a consequence of photodesorption from the chamber walls. All the microbalance results shown in this Letter have considered this.

The specular reflectance spectra of the ice films were collected at an incident angle of 35° with a Fourier Transform infrared spectrometer at 2 cm^{-1} resolution. The reflectance ratio R was obtained by dividing the reflectance spectra by the spectrum of the gold mirror, and then converted to optical depth, $-\ln(R)$. Methods for quantification of the infrared measurements are published elsewhere (Loeffler et al. 2006b).

3. RESULTS

We first deposited a 1600 ML ice film at 70 K and then cooled it to 50 K. After deposition, O_2 gas was leaked into the vacuum chamber to a pressure of 7×10^{-7} mbar, while we monitored the mass uptake by the ice film with the QCM.

After oxygen adsorption reached equilibrium at a level of 8.1 ML, we irradiated the ice at normal incidence. Figure 1 shows that the column density increases during UV irradiation to a saturation at a fluence of $\sim 4.3 \times 10^{19}$ photons cm^{-2}. No mass loss due to desorption was observed when we stopped irradiation and pumped the O_2 from the chamber, contrary to the complete desorption of adsorbed O_2 in non-irradiated ice films, which is consistent with our previous studies (Shi et al. 2009). The total amount of O_2 retained in the ice corresponds to ∼55 ML, which is ∼7 times higher than the equilibrium adsorption in the absence of irradiation.

The total amount of O_2 retained in the ice film increases with decreasing temperature. At 40 K, 166 ML are retained, corresponding to 10.4% of the total column density of the film. For comparison, we measured a ∼21% void space (porosity) in the ice film by UV–visible spectroscopic interference (Teolis 2007). The retention amounts are 55, 19, 12 ML at 50, 70, 78 K, respectively. The initial evolution of the mass uptake (Figure 1, inset) can be well fitted with a quadratic curve, which will be discussed below.

To determine whether the retained oxygen is in the state of molecular O_2 due to UV photon-induced ice compaction or in a compound, such as H_2O_2, formed through photochemical reactions, we first conducted a control experiment of UV

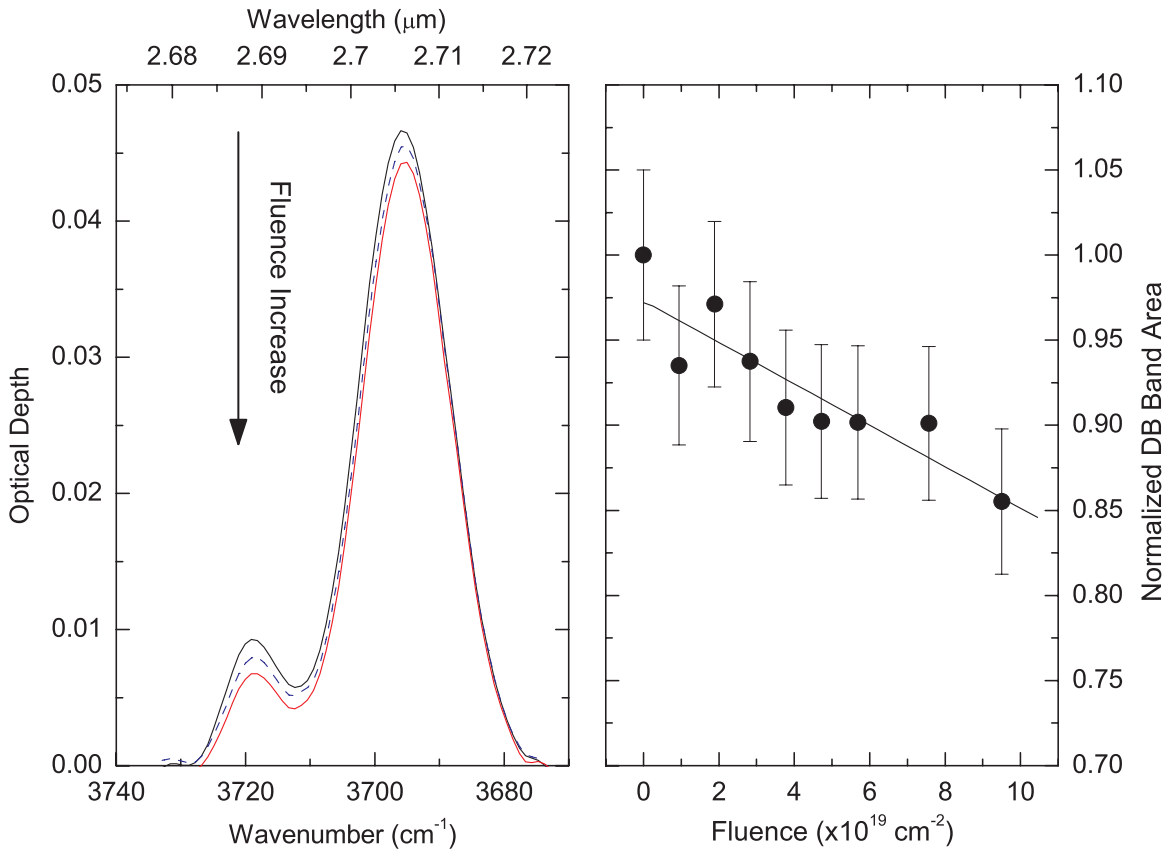

Figure 2. Left: evolution of the OH stretch band due to dangling bonds with fluence for nanoporous ice at 50 K. Right: band area, a measure of porosity, as a function of fluence.

(A color version of this figure is available in the online journal.)

irradiation of a porous ice film without ambient O_2. The only observed change was the small decrease of the dangling bond (DB) absorption at 2.7 μm (Figure 2) due to incompletely coordinated molecules on the pore surfaces. This absorption feature is an indicator of nano-porosity in water ice films (Rowland & Devlin 1991; Raut et al. 2007).

As seen in Figure 2 (right), the normalized area of the DB absorption falls by 6.6% $\pm$ 2.5% by the time we reach the same fluence (4.3×10^{19} photons cm^{-2}) shown in the experiment of Figure 1, corresponding to a destruction cross section of 1.5×10^{-21} cm^2. This value is extremely small because 193 nm is at the absorption edge of H_2O ice (Browell & Anderson 1975; Seki et al. 1981). The cross section is close to the absorption cross section for gaseous water, 1.6×10^{-21} cm^2 (Chung et al. 2001), and orders of magnitude larger than for bulk hexagonal ice (Warren & Brandt 2008), suggesting that the photons are absorbed by less-coordinated surface H_2O, removing the dangling bond, possibly by ejecting an H atom (Yabushita et al. 2004).

Since the fluence that saturates the photo-enhanced gas adsorption (Figure 1) leads to only a 6.6% decrease in the dangling bonds (Figure 2, right panel), the enhanced trapping of oxygen is likely not due to pore collapse and suggest processes where photo-induced reaction of oxygen play a role. A likely process is dissociation of O_2 which, with a cross section of 4.2×10^{-19} cm^2 in the condensed phase (Lu et al. 2008; Raut et al. 2011), is 280 times more likely to absorb 193 nm photons than weakly coordinated water molecule on the surface of a pore.

However, it is possible that even if the pores remain mostly intact, a blockage in the pathways connecting the nanopores in the film to the vacuum may be responsible for increasing gas retention in the ice film. Thus, we conducted additional experiments under the same conditions as those with O_2, but using N_2 and Ar instead, species that do not absorb 193 nm light. Figure 3 shows the amount of gas trapped in the ice films. There is no increase in absorption in both cases and the gases desorb after the ambient pressure is removed. Desorption curves were the same irrespective of irradiation. These experiments suggest that passages connecting nanopores to vacuum are not closed by photon irradiation.

To further stress the importance of photo-induced reactions of O_2, we also performed experiments adsorbing both O_2 and Ar onto 1600 ML ice films. In the first case, we introduced O_2 into the vacuum chamber at a pressure of 7×10^{-7} mbar, waited for the O_2 adsorption to reach equilibrium, and then introduced Ar at a partial pressure of 7×10^{-7} mbar, bringing the total pressure in chamber to 1.4×10^{-6} mbar. After the Ar adsorption equilibrium, we irradiated the film with UV photons until the increase in adsorption saturated. In the second case, we repeated the above experiment except we switched the order of introduction of O_2 and Ar gases. The results show that the increase in mass during UV irradiation was the same for both cases, although initially, the adsorbed ratio of Ar/O_2 is different due to the order in which each gas was dosed. Remarkably, no trapped Ar was found in temperature programmed desorption (TPD) following this set of experiments, indicating that the adsorbed Ar atoms were totally replaced with O_2, and no

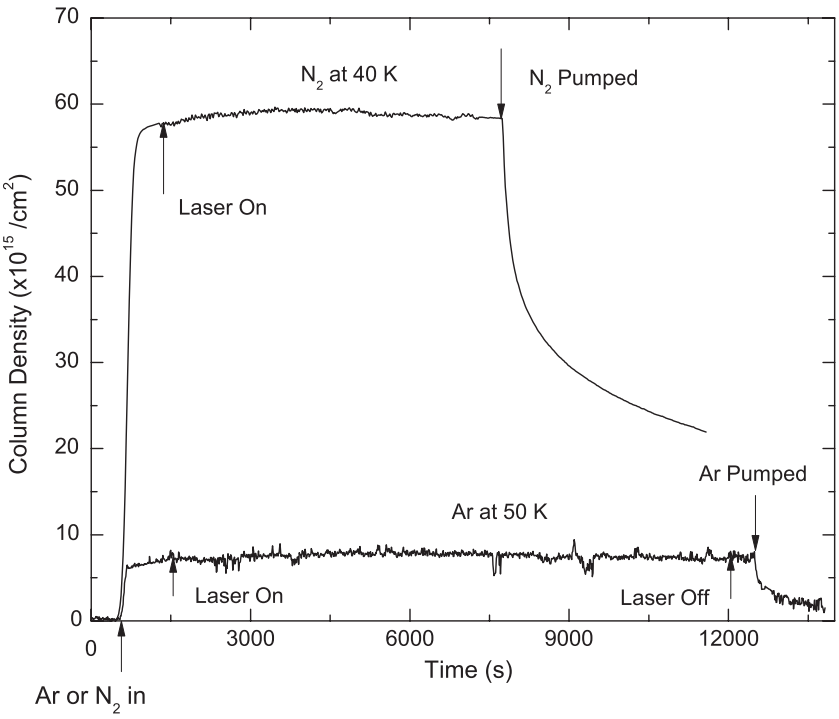

Figure 3. Comparison of the evolution of column density during experiments with ambient Ar and N_2 gas. The 1600 ML ice films were irradiated at 40 K and 50 K for N_2 and Ar, respectively. Irradiation was started after adsorption equilibrium.

passages open to vacuum were blocked due to UV irradiation, since, otherwise, Ar would have remained trapped and released above 140 K following crystallization. Thus, we conclude that the retention of O_2 following irradiation is not due to ice compaction, but due to photo-induced chemical reactions with adsorbed O_2 induced by the 193 nm photons.

This conclusion was confirmed by two independent measurements in ice irradiated in ambient O_2. Infrared absorption spectra showed the presence of O_3 at 1037 cm^{-1} and H_2O_2 at 2855 cm^{-1} at 40 K and thermal desorption after irradiation showed no evidence of trapped O_2. We find that the amount of both molecules decreases as the temperature increases (Figure 4), which is consistent with a lower concentration of adsorbed O_2 in the sample, as expected from the exponential decrease in the quantity of O_2 adsorbed in nanopores with increasing ice temperature (Shi et al. 2009). In addition, we find that the H_2O_2 band shifts from 2855 to 2865 cm^{-1} between 40 K and 78 K. Finally, we note that at 40 K we observed a small infrared absorption peak at ~1250 cm^{-1}, likely due to HO_3 (Cooper et al. 2006; Loeffler et al. 2006a).

Interestingly, the shape and position of the H_2O_2 absorption band at 3.5 μm is consistent with this molecule being surrounded by water ice (Loeffler & Baragiola 2005). The H_2O_2 band shifts from 2855 to 2865 cm^{-1} between 40 K and 78 K. The decrease in concentration from 21% at 40 K to 1.5% at 78 K reflects the decrease in the initial absorption of O_2.

4. DISCUSSION

The energy of the UV photons used in these experiments, 6.4 eV, is higher than the dissociation energy of O_2 (5.1 eV). As we mentioned above, the absorption of these photons by pure ice is extremely unlikely. At lower temperatures, more O_2 is adsorbed in the nanopores of the ice film, resulting in a higher probability for O_3 formation. The ratio of ozone to O_2 concentration at 193 nm is ~0.07 for pure O_2 or ozone solids (Raut et al. 2011) and is smaller in the presence of water.

The *Galileo* NIMS infrared spectra data helped identify H_2O_2 on Europa (Carlson et al. 1999), through the 3.5 μm absorption band. The presence of H_2O_2 was attributed to the radiation processing of the surface ice by magnetospheric ions (Gomis et al. 2004a, 2004b; Pan et al. 2004; Loeffler et al. 2006a, 2006b; Zheng et al. 2006). The mechanism is thought to be dissociation of water, followed by out-diffusion of H leaving an oxygen enriched ice, with a lower probability for the back reaction H + OH → H_2O and therefore an increased likelihood of OH + OH → H_2O_2 reactions (Teolis et al. 2009). The H_2O_2 production by ion impact is found to decrease with increasing temperature and is attributed to the competing phenomena of OH diffusion away from the ion track and hydrogen escape from the ice so that H_2O_2 production at higher temperatures is less efficient due to higher H escaping rate.

The results of this study show an additional mechanism for production of hydrogen peroxide and ozone on icy bodies. Another mechanism leading to formation of O_3 is through decomposition of H_2O_2 (Loeffler et al. 2006a), however, in this study, we are unable to evaluate the relative importance of the two mechanisms leading to O_3 formation, i.e., O/O_2 combination and H_2O_2 decomposition.

When ambient O_2 is present, another pathway of synthesis of H_2O_2 may be through reactions of H_2O with a trapped O atom from photodissociation of adsorbed O_2:

$$O + H_2O \rightarrow OH\text{–}HO. \quad (1)$$

If the hydroxyl radicals would then react to form H_2O_2, there would be a linear mass uptake with irradiation time. However, Figure 1 shows that the initial dependence is quadratic, indicating that two photons are required to form hydrogen peroxide. For instance, another photon absorbed by the 2OH complex could rearrange the atoms to their positions (HO–OH)

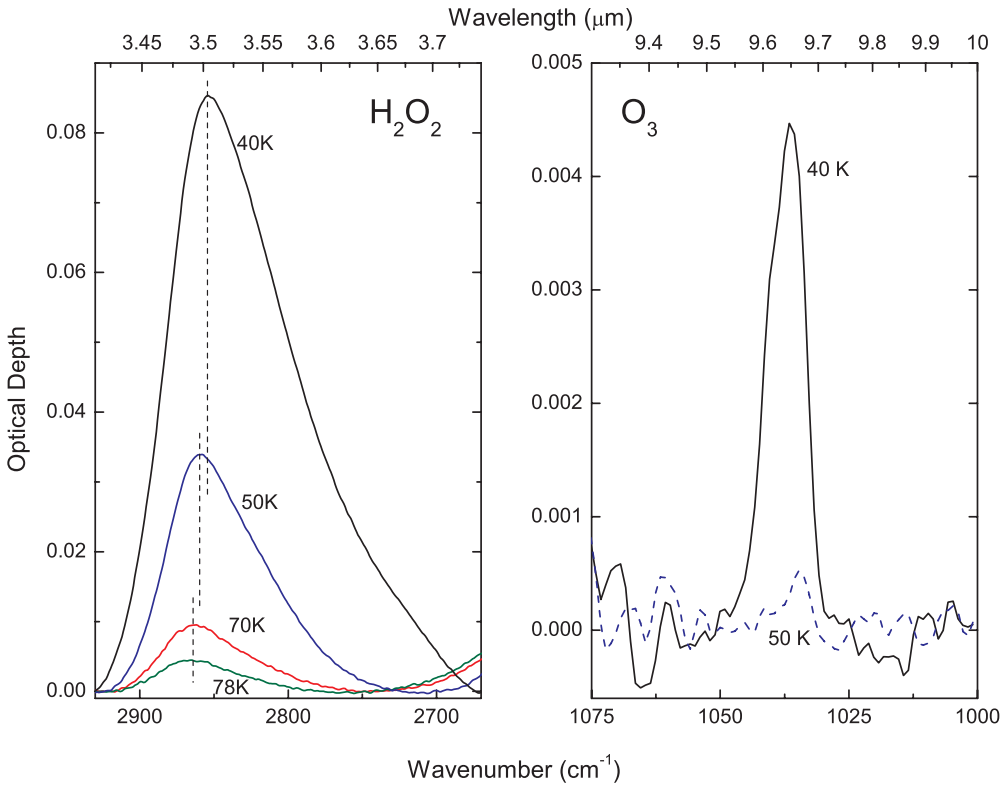

Figure 4. Absorption bands of hydrogen peroxide and ozone for films at 40 K and 50 K in ambient O_2 to a photon fluence of 5×10^{19} photons cm^{-2}. (A color version of this figure is available in the online journal.)

in the H_2O_2 molecules. The exothermic reaction (1) will be favored if the O atoms find a dangling H at the surface of the nanopores, thus the production of H_2O_2 will consume the dangling bonds that give rise to the DB absorption band.

In this scheme, one adsorbed O_2 can be converted into two H_2O_2 if no O_3 formation occurs and thus the number of H_2O_2 produced will be twice the enhanced gas uptake. Although ozone is also formed, both from photolysis of adsorbed O_2 or from decomposition of H_2O_2 (Loeffler et al. 2006a), the proportion is <3% of that of H_2O_2. Thus, ~332 ML of hydrogen peroxide are formed from 166 ML of O_2 in the 1600 ML ice film at 40 K.

5. ASTROPHYSICAL IMPLICATIONS

The process for UV photosynthesis of hydrogen peroxide and ozone described here could take place at icy satellites in the outer solar system, particular in Saturn's ring environment, where oxygen is abundant (Young et al. 2005; Waite et al. 2005) and where UV photon irradiation is believed to be the dominant radiolytic agent (Johnson & Quickenden 1997). UV photons with wavelengths above the water absorption edge can penetrate ice much deeper (~2 m for 193 nm photons) than ionizing radiation or Lyα photons. Thus, they can produce radiation effects deeper in the surface than previously considered.

Our results are extensible to the loose grain structure believed to exist in icy regoliths due to micrometeorite impact comminution. The space between these icy grains result in macroporosity, which can significantly increase the residence time of adsorbed molecules such as O_2. Although this regolith macroporosity is different from nanoporosity that develops in vapor-deposited ice films (discussed here), dangling water molecules also will occur on its surfaces. An O_2 molecule trapped on those internal macropore surfaces meters below the surface could be dissociated by solar photons resulting in O atoms to react with dangling H_2O to synthesize peroxide as demonstrated in this study.

The enhanced depth of penetration of the UV light has other consequences. It has been suggested that the habitability of the putative subsurface ocean beneath may depend on the delivery of radiolytic oxidants produced on Europa's icy crust (Hand et al. 2006). The O_2 loading from the ice shell into the ocean based on a surface abundance of H_2O_2 (0.13% by number relative to ice) is estimated to be $\sim 10^9$–10^{12} molecules yr^{-1} (Chyba & Hand 2001). Here, we have demonstrated that the production of H_2O_2 is significantly enhanced from irradiation of porous ice in the presence of ambient O_2. Furthermore, H_2O_2 production can occur to depths of meters (Warren & Brandt 2008) by 193 nm photons, many orders of magnitude deeper than can be achieved by magnetospheric ions (Cooper et al. 2001). Given the presence of condensed O_2 on the surface of Europa (Spencer & Calvin 2002), it is possible that the H_2O_2 is being formed meters below the ice surface and at higher concentration via the new mechanism described here.

This research was supported by NASA Planetary Atmospheres and NSF Astronomy.

REFERENCES

Bahr, D. A., Famá, M., Vidal, R. A., & Baragiola, R. A. 2001, J. Geophys. Res., 106, 33285
Baragiola, R. A. 2003, Planet. Space Sci., 51, 953
Browell, E. V., & Anderson, R. C. 1975, J. Opt. Soc. Am., 65, 919
Calvin, W. M., Johnson, R. E., & Spencer, J. R. 1996, Geophys. Res. Lett., 23, 673
Carlson, R.W., Anderson, M. S., Johnson, R. E., et al. 1999, Science, 283, 2062
Chung, C.-Y., Chew, E. P., Cheng, B.-M., Bahou, M., & Lee, Y.-P. 2001, Nucl. Instrum. Methods Phys. Res. A, 467–468, 1572
Chyba, C. F., & Hand, K. P. 2001, Science, 292, 2026

Cooper, J. F., Johnson, R. E., Mauk, B. H., Garrett, H. B., & Gehrels, N. 2001, Icarus, 149, 133
Cooper, P. D., Moore, M. H., & Hudson, R. L. 2006, J. Chem. Phys., 110, 7985
Gomis, O., Leto, G., & Strazzulla, G. 2004a, A&A, 420, 405
Gomis, O., Satorre, M. A., Strazzulla, G., & Leto, G. 2004b, Planet. Space Sci., 52, 371
Hand, K. P., Chyba, C. F., Carlson, R. W., & Cooper, J. F. 2006, Astrobiology, 6, 463
Hardwick, T. J. 1952, Can. J. Chem., 30, 23
Hendrix, A. R., Barth, C. A., Stewart, A. I. F., Hord, C. W., & Lane, A. L. 1999, in 30th Annual Lunar and Planetary Science Conference (Houston: Lunar Planetary Institute), abstract no. 2043
Johnson, R. E., & Jesser, W. A. 1997, ApJ, 480, L79
Johnson, R. E., Luhmann, J. G., Tokar, R. L., et al. 2006, Icarus, 180, 393
Johnson, R. E., & Quickenden, T. I. 1997, J. Geophys. Res., 102, 10985
Jurac, S., Johnson, R. E., & Richardson, J. D. 2001, Icarus, 149, 384
Krimigis, S. M., & the MIMI Team 2005, Science, 307, 1270
Loeffler, M. J., & Baragiola, R. A. 2005, Geophys. Res. Lett., 32, 17202
Loeffler, M. J., Raut, U., Vidal, R. A., & Baragiola, R. A. 2006b, Icarus, 180, 265
Loeffler, M. J., Teolis, B. D., & Baragiola, R. A. 2006a, J. Chem. Phys., 124, 104702
Lu, H.-C., Chen, H.-K., Cheng, B.-M., & Ogilvie, J. F. 2008, Spectrochim. Acta A, 71, 1485
Noll, K. S., Johnson, R. E., Lane, A. L., Domingue, D. L., & Weaver, H. A. 1996, Science, 273, 341
Noll, K. S., Roush, T. L., Cruikshank, D. P., Johnson, R. E., & Pendleton, Y. J. 1997, Nature, 388, 45
Pan, S. N., Bass, A. D., Jay-Gerin, J.-P., & Sanche, L. 2004, Icarus, 172, 521
Raut, U., Loeffler, M. J., Famá, M., & Baragiola, R. A. 2011, J. Chem. Phys., 134, 194501
Raut, U., Teolis, B. D., Loeffler, M. J., et al. 2007, J. Chem. Phys., 126, 1
Rowland, B., & Devlin, J. P. 1991, J. Chem. Phys., 94, 812
Sack, N. J., & Baragiola, R. A. 1993, Phys. Rev. B, 48, 9773
Seki, M., Kobayashi, K., & Nakahara, J. 1981, J. Phys. Soc. Japan, 8, 2643
Shi, J., Teolis, B. D., & Baragiola, R. A. 2009, Phys. Rev. B, 79, 235422
Spencer, J. R., & Calvin, W. M. 2002, AJ, 124, 3400
Spencer, J. R., Calvin, W. M., & Person, M. J. 1995, J. Geophys. Res., 100, 19049
Teolis, B. D. 2007, PhD thesis, Univ. Virginia
Teolis, B. D., Jones, G. H., Miles, P. F., et al. 2010, Science, 330, 1813
Teolis, B. D., Loeffler, M. J., Raut, U., Fama, M., & Baragiola, R. A. 2006, ApJ, 644, L141
Teolis, B. D., Shi, J., & Baragiola, R. A. 2009, J. Chem. Phys., 130, 134704
Teolis, B. D., Vidal, R. A., Shi, J., & Baragiola, R. A. 2005, Phys. Rev. B, 72, 245422
Tokar, R. L., et al. 2005, Geophys. Res. Lett., 32, L14S04
Waite, J. H., Cravens, T. E., Ip, W.-H., et al. 2005, Science, 307, 1260
Warren, S. G., & Brandt, R. E. 2008, J. Geophys. Res., 113, D14220
Yabushita, A., Hashikawa, Y., Ikeda, A., Kawasaki, M., & Tachikawa, H. 2004, J. Chem. Phys., 120, 5463
Young, D. T., Berthelier, J.-J., Blanc, M., et al. 2005, Science, 307, 1262
Zheng, W. J., Jewitt, D., & Kaiser, R. I. 2006, ApJ, 639, 534